Chemical Engineering Journal 454 (2023) 140166

Contents lists available at ScienceDirect

Chemical Engineering Journal

journal homepage: www.elsevier.com/locate/cej

Biological conversion of methane to bioplastics: Kinetics, stoichiometry, and thermodynamic considerations for process optimization

Jorge Luis Meraz [a,*], Anthony J. Abel [b], Douglas S. Clark [b], Craig S. Criddle [a]

[a] Department of Civil and Environmental Engineering, Stanford University, United States
[b] Department of Chemical and Biomolecular Engineering, University of California, Berkeley, United States

ARTICLE INFO

Keywords:
Methane
Methanotrophs
Polyhydroxybutyrate
PHB
Modeling
Bioreactor

ABSTRACT

Bioconversion of methane, a potent greenhouse gas, into biodegradable polyhydroxybutyrate (PHB), is an attractive option for methane management. Aerobic bioreactors designed for α-proteobacterial (Type II) methanotrophs can be operated to enable growth and PHB accumulation under nutrient-limiting conditions when fed CH_4 as their sole source of carbon and energy. Using first principles, we develop and test a dynamic model for growth and PHB accumulation. The model includes the kinetics and stoichiometry of Type II methanotrophs and PHB accumulation, acid/base equilibria, metabolic heat release, and physicochemical transport of gaseous substrates through aqueous media. The model was then validated using an experimental dataset extracted from the literature. The numerical simulation accurately describes growth and PHB accumulation. After model validation, we explored the impacts of gas delivery rate, reactor pressure, metabolic heat release, and pH on productivity and energy efficiency. Our results indicate that high mass-transfer rates and high-pressure operation are not needed to achieve significant PHB productivity, on the order of grams per liter per hour. The model also identifies operational windows that decrease energy inputs for cooling and mass transfer of oxygen and methane while still enabling significant PHB productivity.

1. Introduction

Methane (CH_4) is the second most abundant greenhouse gas and one of the most potent greenhouse gases emitted into the atmosphere with a global warming potential over 20 times that of carbon dioxide (CO_2). It is ubiquitous in both natural and built environments, such as landfills and anaerobic digesters, and has the potential to be a next generation carbon feedstock considering its relative low-cost compared to commonly used sugar feedstocks and their many derivatives [1]. The methanotrophic bacteria that can mediate these transformations include gammaproteobacteria (Type I) methanotrophs and alphaproteobacteria (Type II) methanotrophs. Both organisms can convert CH4 into valuable products at ambient temperatures [2,3]. Of the many products that methanotrophs can generate, polyhydroxyalkanoates (PHAs) are of particular interest as they could potentially replace traditional petroleum-based plastics. PHAs are biodegradable and renewable alternatives to petrochemical plastics and can be used in a wide range of applications, including packaging, medicine, and clothing [4–6].

When CH4 is provided as sole substrate, alphaproteobacteria (Type II) methanotrophs can produce high molecular weight polyhydroxybutyrate (PHB). Other PHAs can also be produced by addition of co-substrates, such as valerate. These features have increased interest in process fundamentals, such as methane mass transfer, optimized nutrient composition, and maximizing product yield [7–9]. While CH_4 is attractive due to its abundance and low-cost, its use is hindered due to explosion risks and low solubility in water. Moreover, methanotroph growth is highly exothermic, requiring cooling and making process scale-up more challenging. Scale-up must address gas delivery, pressure, and heat management. Cost-effective scale-up is limited by the relatively slow growth of methanotrophs, explosion hazards, and mass transfer of sparingly soluble CH_4 and O_2. While several studies have investigated the impacts of increasing solubility and energy input on delivery of CH_4 in aqueous solutions, progress towards scale-up has been limited, due in part to the complex physicochemical and biological kinetic reactions that take place during growth and PHB accumulation. Because all these processes occur simultaneously, they are difficult to track, and optimal control strategies can be overlooked. To overcome this limitation, kinetic growth and substrate models can be used to better understand complex chemical, and thermodynamic reactions while also considering relevant bioreactor physics. A physics-based model is a

* Corresponding author.
E-mail address: jmeraz@stanford.edu (J.L. Meraz).

https://doi.org/10.1016/j.cej.2022.140166

Available online 5 November 2022

useful tool that can be used to optimize PHB production processes and limit the amount of experimentation needed for scale-up and process optimization.

PHB accumulation generally occurs when bacteria are grown under nutrient-deficient conditions where substrates other than the carbon source, typically nitrogen or phosphorus, limit cell division [10–12]. Kinetic models developed to date include PHB production by heterotrophic organisms, with the majority focusing on PHB production via Cupriavidus necator [13–15]. Mozumder et al. 2015 [13] developed several models of PHB production by C. necator under heterotrophic and autotrophic conditions. Autotrophic PHB production is of particular interest because it relies upon efficient delivery of gaseous substrates (e.g., hydrogen (H2), oxygen, carbon dioxide). Their model accurately described autotrophic growth and PHB accumulation and enabled a scenario analysis, demonstrating that maximum PHB concentration can be achieved under oxygen stress, as opposed to nitrogen limitation.

To date, few models are capable of simulating methanotrophic growth and PHB accumulation. One such model is that of Moradi et al. [16]. In this model, Methylocystis bacteria in a bubble column reactor produce PHB from natural gas (carbon and electron donor). Model simulations enabled exploration of mass transfer, momentum, and cell density. The model captured kinetic dependencies of air to CH4 ratios for Methylocystis hirsuta, with a maximum biomass concentration of 1.6 g/L and PHB concentration of 0.01 g/L. A model developed by Chen et al. [17] simulated PHB synthesis from biogas (mixture of CH4 and CO2) using *Methylocystis hirsuta*. Their mechanistic model considers several relevant processes such as biomass growth and decay, PHB synthesis, and availability of CH_4 and O_2, including the mass transfer coefficient (k_La). With their model Chen et al. determined that an optimal O_2/CH_4 molar ratio of 1.6 mol O_2 mol^{-1} CH_4 maximized PHB synthesis of *M. hirsuta*. These models, however, did not consider the complex nature of chemical reactions (e.g., acid/base chemistry) that occur when physical constraints are modified (e.g., k_La, pressure). While such studies can simulate methanotrophic growth and PHB accumulation, mathematical models are nonetheless needed to elucidate the thermodynamic and relevant microbial kinetic parameters that can propel this technology to an industrial scale.

In this paper, we present a comprehensive, physics-based modeling approach to maximize PHB synthesis within a well-studied Type II methanotroph, *Methylocystis* spec. GB 25 [11,18,19]. Specifically, we consider the impacts of gas delivery rate, pressure, metabolic heat release, pH, and heat transfer rate on reactor productivity and efficiency. The model is used to simulate and evaluate the effects of each of these operating parameters on key bioreactor performance metrics such as biomass and PHB productivity, titer, and overall energy efficiency. The methodology and analysis provides a generic framework for analyzing and identifying key microbial and reactor characteristics that can maximize PHB production via methanotrophic organisms.

2. Materials and methods

2.1. Stoichiometry & kinetics

The model developed in this work considers two main microbial processes: 1) biomass growth and 2) PHB accumulation. Most stoichiometric yield coefficients and kinetics for *Methylocystis* spec. GB 25 growth and PHB accumulation on CH_4 were taken from [19] and [11]. All of the stoichiometric and kinetic values and parameters listed in the Supplementary materials (Table S1) are summarized in Tables 1, 2 and 3.

2.2. Stoichiometry of growth and PHB

Several studies have evaluated stoichiometric terms for methanotroph growth and PHB accumulation, including oxygen limitation. Typical molar ratios for biomass growth range from 1.4 to 1.8 mol of O_2 consumed per mol of CH_4 consumed; similar molar ratios are reported for PHB accumulation [20–23]. Asenjo & Suk 1986 noted that the theoretical maximum yield of biomass growth on CH4 is 0.65 g biomass/g CH4, whereas for PHB the maximum yield is 0.67 g PHB/g CH4. For biomass and PHB yield, the values are estimated based on the serine cycle (Type II methanotrophs) and assuming that ammonia is the nitrogen source. For model validation, experimental yield values of biomass growth and PHB accumulation were obtained from Wendlandt et. al. [11,19]. Growth yield for Methylocy*stis* spec. GB 25 is noticeably higher than calculated theoretical yields, showing the diverse nature of CH_4 consumption across methanotrophic organisms.

2.3. Kinetics of growth

The first phase of the model developed in this work considers biomass growth using Monod kinetics. Growth requires gaseous substrates (CH_4, O_2, CO_2) and liquid substrate ammonium-nitrogen (N). For individual substrate kinetic expressions, there are associated half-saturation constants (K_i) and inhibition constants (KI_i), each described in Table S1 in Supplementary materials. Liquid-phase ammonia and ammonium concentrations can inhibit growth above concentration thresholds for methanotrophs, but the levels used here in modeling are kept below the thresholds. Biomass growth is limited by low-levels of ammonium-N in the liquid phase; that is, the biomass shifts from a period of active biomass growth to phase 2, PHB accumulation. Aqueous concentrations of CO_2 are included in both phases based upon evidence that CO_2, whether added as gas or bicarbonate, shortens the initial lag phase; however high concentrations inhibit growth, especially at elevated pressures [19,24]. Moreover, CO2 impacts bioreactor pH and microbial growth as predicted by acid/base chemistry and microbial dependence upon pH, detailed in the following sections [25].

2.4. Kinetics of PHB accumulation

The concentration of nitrogen in the growth medium functions as a switch that controls which phase of the overall process dominates. If the extracellular nitrogen concentration is too high ($N > K_{IN}$), both biomass growth and PHB accumulation are inhibited. Accordingly, if the extracellular nitrogen concentration is less than K_{IN}, but greater than K_{PIN} (concentration above which no PHB accumulates), the specific growth rate of active biomass exceeds the specific rate of PHB synthesis, and growth is balanced. For this analysis the K_{PIN} value is assumed to be equivalent to K_N. When extracellular nitrogen concentration is less than K_{PIN}, growth is unbalanced, biomass growth decreases, and PHB accumulates.

PHB accumulation is described by modified Monod kinetic expressions, as described previously by Asenjo & Suk 1986 [21,26]. Conditions for PHB accumulation of methanotrophic organisms require that CH4 and O2 are supplied in excess; to maintain this environment CH4 and O2 are constantly fed into the reactor while PHB accumulation occurs [21].

Table 1
Stoichiometry for growth and PHB accumulation.

Component → Process ↓	CH_4 [gL^{-1}]	O_2 [gL^{-1}]	NH_4-N [gL^{-1}]	CO_2 [gL^{-1}]	Active Biomass, X_a [gL^{-1}]	PHB, X_{PHB} [gL^{-1}]
Biomass Growth	$-1/Y_{x,CH4}$	$-1/Y_{x,O2}$	$-1/Y_{x,N}$	$Y_{x,CO2}$	1	
PHB Accumulation	$-1/Y_{p,CH4}$	$-1/Y_{p,O2}$		$Y_{p,CO2}$		1

Table 2
Kinetic expressions for growth and PHB accumulation.

Process	Reaction expression	
Biomass growth	$r_x = \mu_x X_a$, where $\mu_x = \mu_{max}\left(\frac{CH_4}{K_{CH_4} + CH_4}\right)\left(\frac{O_2}{K_{O_2} + O_2}\right)\left(\frac{CO_2}{K_{CO_2} + CO_2 + \frac{CO_2}{K_{ICO_2}}}\right)\left(\frac{N}{K_N + N}\right)$	(1)
PHB Accumulation	$r_p = \mu_P X_{PHB}$, where $\mu_p = \mu_{p,max}\left(\frac{CH_4}{K_{CH_4} + CH_4}\right)\left(\frac{O_2}{K_{O_2} + O_2}\right)\left(\frac{K_{PIN}}{K_{PIN} + N}\right)\left(1 - \left(\frac{P}{P_{max}}\right)^n\right)$	(2)

Table 3
Carbonate acid/base reactions.

Kinetic expression	Equilibrium constant	
$CO_{2_{(aq)}} + H_2O\ k_{+1} \rightleftharpoons k_{-1}\ H^+ + HCO_3^-$	K_1	(10)
$HCO_3^- k_{+2} \rightleftharpoons k_{-2}\ H^+ + CO_3^{2-}$	K_2	(11)
$CO_{2_{(aq)}} + OH^-\ k_{+3} \rightleftharpoons k_{-3}\ HCO_3^-$	$K_3 = K_1/K_w$	(12)
$HCO_3^- + OH^-\ k_{+4} \rightleftharpoons k_{-4}\ CO_3^{2-} + H_2O$	$K_2 = K/K_w$	(13)
$H_2O\ k_{+w} \rightleftharpoons k_{-w}\ H^+ + OH^-$	K_w	(14)

The kinetics of PHB accumulation are described by the asymptotic product inhibition Equation 2 in Table 2. This expression takes into consideration that cells are not capable of producing PHB in an unlimited manner, but that PHB accumulation rate slows down as the ratio of PHB to active biomass, P_{max}, approaches its maximum value (set by experimental results from Helm 2002 [26], and Wendlandt, et al. 2001 [11], see Supplementary Table S1). The dimensionless fitting parameter,n, is an exponent that describes the time dependence of product accumulation within the cell, in this case, PHB, and can range from 0 to > 1, depending on the type of inhibition [21,27].

2.5. Metabolic heat release, $\triangle_c H_{met}$

Critical to process design and scale-up of methanotrophic processes is heat management. Aerobic methanotrophic growth is highly exothermic [22,28]. Compared to abiotic combustion of CH_4, biological oxidation of CH_4 results in the release of $\sim$ 72 % of the total heat released relative to burning CH_4 alone. A detailed analysis of this calculation can be found in [22].

Taking a similar approach to El Abbadi and Criddle 2019 [22], the accumulation of PHB releases close to 80 % of the heat released by abiotic combustion of CH_4. Heat released during PHB synthesis is calculated as follows:

$$\triangle_c H_{met} = \triangle_c H_{CH_4} - fs \triangle_c H_{PHB} \tag{3}$$

where $\triangle_c H_{met}$ [kJgCOD^{-1}] is the specific heat of metabolism, and $\triangle_c H_{CH_4}$ [kJgCOD^{-1}] and $\triangle_c H_{PHB}$ [kJgCOD^{-1}] are the specific heats of combustion for CH_4 and PHB, respectively. $fs_{PHB}[-]$ represents the fraction of electrons from CH_4 that are routed towards PHB synthesis and is described as:

$$fs_{PHB} = Y_{PHB} * \frac{\gamma_{COD}}{\gamma_{PHB}} * \frac{\gamma_{CH_4}}{\gamma_{COD}} \tag{4}$$

where Y_{PHB} is the yield of PHB [$g_{PHB}g_{CH4}^{-1}$], $\frac{\gamma_{COD}}{\gamma_{PHB}}$ [$g_{COD}g_{PHB}^{-1}$] is the chemical oxygen demand (COD) to weight ratio of PHB, and $\frac{\gamma_{CH_4}}{\gamma_{COD}}$ [$g_{CH4}g_{COD}^{-1}$] is the COD to weight ratio of CH_4.

Heat release due to growth and PHB accumulation must be accounted for in bioreactor design, especially at high cell densities, where it can increase temperature and decrease the solubility of dissolved CH_4 and dissolved O_2. Moreover, heat management is critical to maintain high productivity rates as unregulated temperatures (e.g., too high or too low) are likely to negatively impact maximum specific growth rates. For our model, we assume that heat generated is based on the stoichiometry of metabolic heat release for growth and PHB accumulation. No other major sources of heat were considered for this analysis.

2.6. Microbial growth dependence on temperature and pH

A simple model developed by Rosso et al. 1995 [25] and utilized in Abel and Clark 2021 [29] is used to describe the effects of temperature and pH on microbial growth and PHB accumulation:

$$\mu_i = \mu_{i,opt}\tau(T)\rho(pH) \tag{5}$$

where $\mu_{i,opt}$ is the growth or PHB accumulation rate at optimal conditions, and $\tau(T)$ and $\rho(pH)$ are described as follows:

$$\tau(T) = \begin{cases} 0, & T < T_{min} \\ f(T), & T_{min} \leqslant T \leqslant T_{max} \\ 0, & T > T_{max} \end{cases} \tag{6}$$

$$\rho(pH) = \begin{cases} 0, & pH < pH_{min} \\ f(pH), & pH_{min} \leqslant pH \leqslant pH_{max} \\ 0, & pH > pH_{max} \end{cases} \tag{7}$$

In these expressions $T_{min/max}$ and $pH_{min/max}$ are the ranges of temperature and pH over which microbial activity is observed and the functions $f(T)$ and $f(pH)$ are:

$$f(T) = \frac{(T_{max} - T)(T - T_{min})^2}{(T_{opt} - T_{min})\left[(T_{opt} - T_{min})(T - T_{opt}) - (T_{opt} - T_{max})(T_{opt} + T_{min} - 2T)\right]} \tag{8}$$

$$f(\mathrm{pH}) = \frac{(\mathrm{pH} - \mathrm{pH_{min}})(\mathrm{pH} - \mathrm{pH_{max}})}{(\mathrm{pH} - \mathrm{pH_{min}})(\mathrm{pH} - \mathrm{pH_{max}}) - (\mathrm{pH} - \mathrm{pH_{opt}})^2} \tag{9}$$

where T_{opt} and pH_{opt} are the optimal temperature and pH over which *Methylocystis* growth and PHB accumulation are observed [30].

2.7. Acid/Base reactions

The primary acid/base reactions we are interested in are those of the carbonate system. These reactions are of interest because CO_2 is released as a byproduct of microbial growth and can inhibit growth if its aqueous concentration exceeds the inhibition CO_2 concentration, K_{ICO2}. All acid/base reactions are described as kinetic expressions and without

assuming equilibrium [29]. Moreover, we consider gas substrate composition when CO_2 is added as a gas. When CO_2 is added as either a gas or as bicarbonate, it helps to shorten the initial lag phase of methanotrophic growth [24]. Typical partial pressures of CO_2 are added in the range of 0–10 % by volume. In the model we evaluate the combined effects of CO_2 from addition as a gaseous substrate and as a byproduct of microbial growth and PHB accumulation.

In the kinetic expressions, k_{+n} and k_{-n} represent the forward and reverse rate constants. K_n is the equilibrium constant that is given by:

$$K_n = exp\left(\frac{\Delta S_n}{R}\right)exp\left(-\frac{\Delta H_n}{RT}\right) \tag{15}$$

Reaction rates for the resulting source and sink terms are computed as:

$$R_{A-B,i} = \sum_n v_i\left(k_{+n}\sum_{v_i<0} c_i - k_{-n}\sum_{v_i>0} c_i\right) \tag{16}$$

where v_i is the stoichiometric coefficient of species i for a reaction, n. The reverse rate constants are calculated by the following relationship:

$$k_{-n} = \frac{k_{+n}}{K_n} \tag{17}$$

2.8. Gas delivery

Mass of gas substrate entering the reactor is described by the ideal gas law:

$$p_i V = n_i RT \tag{18}$$

where p_i is the pressure [atm], V is assumed as a unit volume, R is the universal gas constant and T [℃] is temperature. CH_4, O_2, and CO_2 are delivered at different partial pressures. To account for this, we multiply the total pressure,p_i, by the molar fraction of gas delivered,y_i, to obtain the partial pressure of each gas, and subsequently the total mass (e.g., moles, grams) of gas delivered at various pressure and temperature ranges. The resulting gas phase mass transfer is described below:

$$r_{gas,i} = \frac{D_{gas}}{RT}\left(y_i p_{f,i} - p_i\right) \tag{19}$$

where $r_{gas,\ i}$ [molL^{-1}h^{-1}] is the rate of gas delivery for each gaseous component, D_{gas} is the gas dilution rate [h^{-1}], and $p_{f,i}$ and p_i are the gas feed and bioreactor gas pressures, respectively.

2.9. Gas liquid mass transfer

Equilibrium solubility of gases into the liquid phase is described using the ideal gas law and Henry's constant. From our gas delivery rate equations, using the bioreactor gas phase pressures,p_i, we can derive the aqueous saturation concentration of each gaseous component:

$$C_{sat,i} = \frac{p_{i^*R^*T}}{H_{C_i}} \tag{20}$$

where H_{C_i} is Henry's constant for each gas component. We then define our liquid side mass transfer equations:

$$r_{g-L,i} = k_L a_i\left(C_{sat,i} - C_{i,L}\right) \tag{21}$$

where $r_{g-L,i}$ is the rate of gas transfer to the liquid phase [molL^{-1}h^{-1}], $C_{i,L}$ [molL^{-1}] is the aqueous concentration of gas that is bioavailable (e.g., CH_4, O_2) to bacteria during growth and PHB accumulation.

2.10. Mass transfer Coefficient, k_La

A range of values for volumetric mass transfer coefficients for O_2 (k_La_{O2}) was evaluated assuming previously measured values for several reactor configurations [9]. Using the two resistance and penetration theories, the volumetric mass transfer coefficients for CH4 and CO2 are then estimated using the kLa of O2. Briefly, using the two-resistance theory, the overall mass transfer coefficient is defined as [31]:

$$\frac{1}{k_L a} = \frac{1}{k_L}*\frac{1}{a} = \left(\frac{1}{H^*k_G}*\frac{1}{k_l}\right)*\frac{1}{a} \tag{22}$$

where k_L is the overall gas–liquid mass transfer coefficient [mh^{-1}], a is the gas–liquid interface area [m^{-1}], H is Henry's constant [−], k_G is the gas phase mass transfer coefficient [mh^{-1}], and k_l is the liquid phase mass transfer coefficient [mh^{-1}]. Due to the low water solubility of these gas compounds, gas transfer into the bulk liquid is considered liquid-phase mass transfer controlled and it can be assumed that:

$$H^*k_G \gg k_l \tag{23}$$

Equation (22) can then be rewritten as:

$$k_L a = k_l{}^* a \tag{24}$$

Because each gas substrate shares the same specific interfacial area, gas volumetric mass transfer coefficients only differ relative to their specific liquid mass transfer coefficient, k_l. Moreover, because the system is completely mixed (i.e., intense agitation), the liquid phase mass transfer coefficient exhibits behavior that is consistent with penetration theory [9,32,33]:

$$k_l \propto \sqrt{D_i} \tag{25}$$

where D_i is the aqueous phase diffusion coefficient. Equations 24 and 25 are then combined to give:

$$k_L a_i = \sqrt{\frac{D_i}{D_{O_2}}}*k_L a_{O_2} \tag{26}$$

where k_La and the diffusion coefficient in the numerator change for each gas, i.

2.11. Mass balances

Substrate and CO_2 mass balances of biomass growth and PHB accumulation are expressed as follows:

$$R_{CH_4} = k_L a_{CH_4}\left(CH_{4,sat} - CH_{4_L}\right) - \left(\frac{\mu_x}{Y_{x_{CH4}}} + \frac{\mu_p}{Y_{p_{CH4}}}\right)X \tag{27}$$

$$R_{O_2} = k_L a_{O_2}\left(O_{2,sat} - O_{2_L}\right) - \left(\frac{\mu_x}{Y_{x_{O2}}} + \frac{\mu_p}{Y_{pO2}}\right)X \tag{28}$$

$$R_N = -\left(\frac{\mu_x}{Y_{x_N}}\right)X \tag{29}$$

$$R_{CO_2} = \left(Y_{CO2_{,x}}\right)r_x + \left(Y_{CO2_{,p}}\right)r_p \tag{30}$$

where R_{CH_4} and R_{O_2} are the mass balances on CH_4 and O_2 for the system and contain both the substrate mass delivery rates (result of equations 18–21) and the subrate consumption rates. R_{CH_4} and R_{O_2} consumption rates include consumption from active biomass owth and PHB accumulation, whereas ammonia–nitrogen consumption,R_N, is only impacted by active biomass growth. Substrate consumption is defined by dividing μ_x [h^{-1}] and μ_p [h^{-1}], by the appropriate methanotrophic yield for each substrate of interest (e.g., CH_4, O_2, NH_4-N), where μ_x [h^{-1}] and μ_p [h^{-1}] are the specific rates of biomass growth and PHB accumulation, respectively. X [molL^{-1}] denotes total biomass concentration, which accounts for active biomass,X_a, and PHB, X_{PHB}. R_{CO_2} is the mass balance on carbon dioxide, which is a byproduct of active biomass growth and PHB accumulation. r_x and r_p [molL^{-1}h^{-1}] are the volumetric rates of biomass growth and PHB accumulation (Table 2).

2.12. System energy balance

The energy balance for this system involves a heat source and sink defined as:

$$R_Q = Q_{met} - Q_{exch} \tag{31}$$

where Q_{met} is metabolic heat and Q_{exch} is the heat exchanger, both expressed in units of watts. The heat source is the combined metabolic heat from growth and PHB accumulation and takes on the form:

$$Q_{met} = \left(\triangle_c H_x * \frac{\mu_x}{Y_{x_{CH4}}} * X_a + \triangle_c H_{PHB} * \frac{\mu_p}{Y_{pCH4}} * X_{PHB} \right) * V \tag{32}$$

where $\triangle_c H_x$ and $\triangle_c H_{PHB}$ are the specific heats of combustion for biomass and PHB, respectively. The heat sink of the system (i.e., heat exchanger with cooling agent) is defined as:

$$Q_{exch} = U * A_c * \left(T_{opt} - T_{sys} \right) \tag{33}$$

where U is the overall heat transfer coefficient [$Wm^{-2}{}^{\circ}C^{-1}$], A_c is the cross-sectional area of heat transfer (assumed as 1 [m^2]), T_{opt} [℃] is the optimal temperature of the system and T_{sys} [℃] is the dynamic system temperature. Within the system, the generated metabolic heat increases system temperature,T_{sys}. To manage this increase in heat, a heat exchanger must be able to remove heat at a greater rate than what is generated. The overall heat transfer coefficient is varied within the model to assess the operating range that allows for adequate PHB productivity, titer, and energy efficiency.

2.13. Reactor performance metrics

2.13.1. Productivity

Volumetric productivity is critical to improving cultivation strategies for methanotrophic organisms, in particular, this metric is useful when considering bioreactor scale up. In our model, PHB productivity is assessed to determine optimal bioreactor operational characteristics that allow for productivity near or at the level of grams per liter per hour. Productivity of PHB is calculated by multiplying X_{PHB}, by the specific rate of PHB formation,μ_p.

$$r_p = \mu_p * X_{PHB} \tag{34}$$

2.13.2. Rate limitations

To assess rate-limitations, we calculated a modified Damköhler (Da) number as previously published in Myung et al. 2016 [7]. Briefly, the Da number is defined as the theoretical maximum CH_4 utilization rate (MUR_{Max}) divided by the maximum mass transfer rate (MTR_{Max}):

$$Da = \frac{MUR_{max}}{MTR_{max}} = \frac{q_{max,CH_4} X}{k_L a * C_{sat,CH4}} \tag{35}$$

where q_{max,CH_4} [$g_{CH4} g_{VSS}^{-1} h^{-1}$] is the specific rate of methane utilization, a quantity that is calculated by dividing the specific rates of growth or accumulation by the respective yield for growth or product accumulation. In our simulations methane is consumed by both active biomass growth and PHB formation, both processes are considered within this calculation. The Da number compares the reaction rate (cell metabolism) relative to the transport rate (gas delivery). The ratio of these rates indicates whether a system is limited by cell metabolism (Da ≪ 1) or mass transfer (i.e., Da ≫ 1).

2.13.3. Energy efficiency

Energy efficiency of PHB production is a function of time in a batch process. Continuous efficiency (η_{PHB}) is defined as:

$$\eta_{PHB} = \frac{\left| r_p \Delta H^{\circ}_{c,PHB} \right|}{\left| R_{CH_4} \Delta H^{\circ}_{c,CH4} \right| + P_{kLa}} \tag{36}$$

where, r_p [$molL^{-1}h^{-1}$] is the volumetric rate of PHB production, R_{CH4} [$molL^{-1}h^{-1}$] is the volumetric rate of CH_4 consumption, $\Delta H^{\circ}{}_C$ is the heat of combustion for the product (PHB) or reactant (CH_4), and P_{kLa} is the power requirement for gas–liquid mass transfer and mixing. P_{kLa}, is calculated by rearranging the correlation developed by Klass Van't Riet for stirred vessels [34]:

$$k_L a_{O_2} = 2.6 * 10^{-2} (P_{kLa})^{0.4} (u_G)^{0.5} \tag{37}$$

where k_La_{O2} is the gas–liquid mass transfer coefficient for oxygen [h^{-1}] and u_G is the gas velocity [ms^{-1}] and P_{kLa} has units of [Wm^{-3}]. Power is calculated by assuming a U_G of 0.05 [ms^{-1}]. The k_La is adjusted as described previously within the text. Briefly, the k_La is multiplied by the ratios of the square roots of the respective diffusivities (D) for the gases of interest. For our energy efficiency analysis we consider the diffusivities of O_2 and CH_4.

2.14. Model metrics and implementation

2.14.1. Predictive capability

Model predictive capability is assessed using the Nash-Sutcliffe Efficiency (NSE) factor. This value quantitatively describes model accuracy and has been used in previous modeling efforts [13]. The efficiency factor is described as:

$$E = 1 - \frac{\sum_{i=1}^{t} \left(y_i(t) - y_i^m(t) \right)^2}{\sum_{i=1}^{t} \left(y_i(t) - \underline{y} \right)^2}. \tag{38}$$

NSE factor ranges from $-\infty$ to 1. An efficiency factor of 1 indicates a perfect match between the model and observed results, where a value of 0 indicates that model results are as accurate as the mean of the observed data. Any value below 0 indicates that the observed mean is a better predictor than the model. The closer the efficiency factor is to 1, the more accurate the model.

2.14.2. Model implementation

Model equations are solved using the MUMPS general solver in COMSOL Multiphysics 5.5. The mesh settings are set to allow for a physics-controlled mesh with extremely fine element sizes. All model parameters can be found in Table S1 of the Supplementary Materials.

2.15. Model assessment

To assess model accuracy and predictive capability, we compared our simulated results with an independent literature dataset reported by Wendlandt et al. 2001 [11,12]. All reactor parameters (e.g., pressure, temperature, initial pH, molar O_2/CH_4 ratios) were replicated in the model. Microbial kinetic parameters were taken directly from Wendlandt et al. 2001. When not readily available, kinetic parameters reported in other literature datasets were used (listed in Table S1). In the study used for model validation, PHB production occurred under nitrogen limitation. This limitation is one of the most common strategies used to induce PHB production for PHB accumulating organisms [10,11,13].

2.15.1. Data collection

When not reported, data for biomass and PHB concentrations were collected by digitizing graphs with pertinent data using the WebPlotDigitizer [35], a graphical web-based tool. The software allows for extraction of numerical data from graphs.

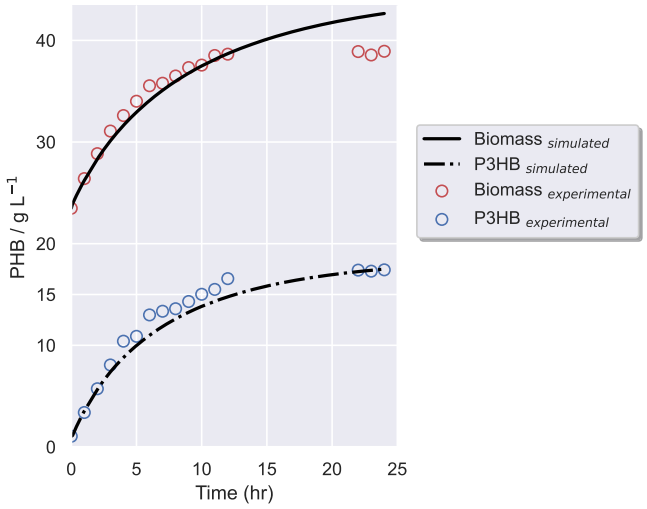

Fig. 1. *Methylocystis spec. GB 25* model validation results.

2.15.2. Model validation

Model validation was carried out assuming that *Methylocystis* GB 25 grows at the specified k_La, pressure, O_2/CH_4 molar ratios, temperature, and pH reported by Wendlandt et al. 2001 [11,12,26]. The model has efficiency factors of 0.85 and 0.90 for total biomass and PHB production, respectively. NSE values above > 0.5 are classified as acceptable, values > 0.75 indicate that the simulated model has a "very good" fit [36].

Fig. 1 describes *Methylocystis* sp. GB 25 growth and PHB production. The model is validated using experimental data from Wendlandt et al. 2001 where nitrogen limitation is used to initiate PHB accumulation. A total pressure of < 0.3 MPa is applied, where the partial pressure of O_2 is $\leqslant 15$ % and that of CH_4 is $\leqslant 20$ %. Total biomass (e.g., Fig. 1 Biomass) is composed of two components: active biomass (RCC) and PHB. Generally, the numerical simulations agree well with the extracted experimental data, with an exception at the end of the experiment. The model overestimates biomass slightly, likely due to metabolic phenomena that are not fully captured. Not shown in the model is the residual cell concentration (RCC) (difference between total biomass and PHB). The RCC does not change much throughout the model (similar to the experimental results), showing that PHB accumulation is essentially a non-growth associated process.

2.15.3. Model ammonium-nitrogen sensitivity analysis

A sensitivity analysis with respect to ammonium-nitrogen concentration was carried out to highlight how nitrogen impacts PHB accumulation. Ammonium mineral salts (AMS) typically contain ~ 10 [mM] ammonium-nitrogen, with nitrogen-limited conditions for PHB accumulation ranging from 2 to 10 [mM]. In some cases, AMS media contains up to 30 [mM] ammonium-nitrogen [37]. In this analysis, we briefly explore the impacts of nitrogen concentration to determine overall impacts on PHB accumulation, and to decide an appropriate level of ammonium-nitrogen for subsequent in-silico experiments. Except for ammonium-nitrogen concentration, all other parameters are similar as those describes previously in 2.15.2.

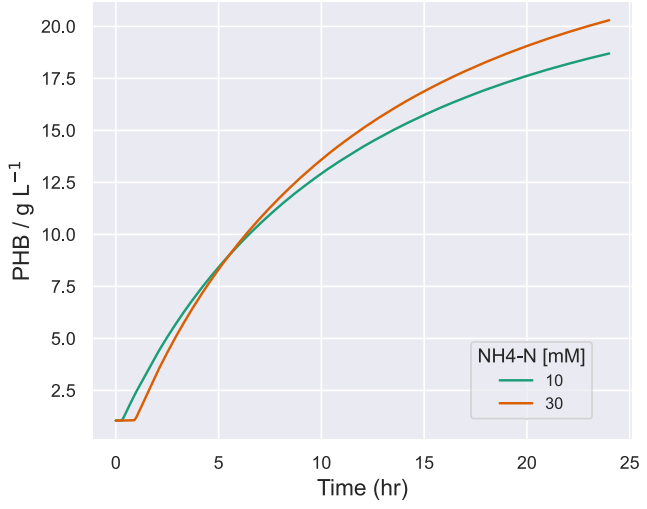

Fig. 2. Model ammonium-nitrogen sensitivity analysis.

Fig. 2 illustrates the impact of varying levels of ammonium-nitrogen on PHB accumulation. 30 [mM] was chosen as the upper bound as this concentration is known to inhibit methane oxidation to some degree [38]. In the figure there is a slight difference in PHB accumulation capabilities, this is expected as higher levels of ammonium-nitrogen allow for more active biomass growth and thus more bacterial cells are available to accumulate PHB. In this in-silico experiment, the difference in PHB accumulation capabilities is minimal, being that 30 [mM] leads to accumulation of ~ 21 [gL^{-1}] as opposed to ~ 18 [gL^{-1}] for the 10 [mM] scenario. This slight difference suggests that lower levels of ammonium-nitrogen are sufficient to reach adequate levels of PHB accumulation, as higher levels may lead to decreased methane oxidation and potentially lower levels of growth and PHB accumulation.

2.16. Experimental roadmap

After model assessment, we evaluate the effects of mass transfer coefficient (k_La), total pressure (P_{tot}), CO_2 partial pressure, temperature, pH, and heat transfer rate on reactor productivity and efficiency. In addition, we evaluated the effects of microbial kinetics on PHB energy efficiency and productivity, considering observed ranges of PHB yield and P_{max} for pure and mixed cultures of methanotrophs. For all subsequent simulations, our experimental design evaluated biomass growth, and PHB titer and productivity using an initial concentration of 10 [mM] ammonium-nitrogen, similar to concentrations used in previous PHB accumulation studies. For each of our simulations we assume a gaseous CH_4 rich environment similar to Wendlandt et al. 2001 [11]. All in-silico experiments were conducted with k_La values ranging from 200 [hr^{-1}] to 1000 [hr^{-1}] and pressures ranging from 1 to 6 atmospheres. When needed, a brief discussion providing further experimental details is included in each subsection of the results and discussion.

3. Results and discussion

3.1. Mass transfer and total pressure impact PHB titer and productivity rates

Many studies have shown that k_La and pressure are important physicochemical parameters for bioreactor design [9,39]. To that end, we used our model to determine the effects of k_La and total pressure on methanotrophic growth and PHB accumulation. To compare across a range of k_La and pressure values, we carried out a parametric sweep over a range of previously reported values. Typical k_La values for bioreactors are in the range of ~ 200–400 h^{-1}. Haynes and Gonzalez noted that a range of 700–1000 h^{-1} is needed to reach productivity rates on the order

Table 4
DamKöhler analysis.

k_La [h^{-1}] → Pressure [atm] ↓	200	300	500	700	1000
1	10	7.8	5	3.5	2.5
2	6	4	2.5	1.8	1.3
3	4	2.8	1.7	1.2	0.8
4	3	2	1.3	0.9	0.6
5	2.5	1.7	1	0.7	0.5
6	2	1.4	0.85	0.6	0.4

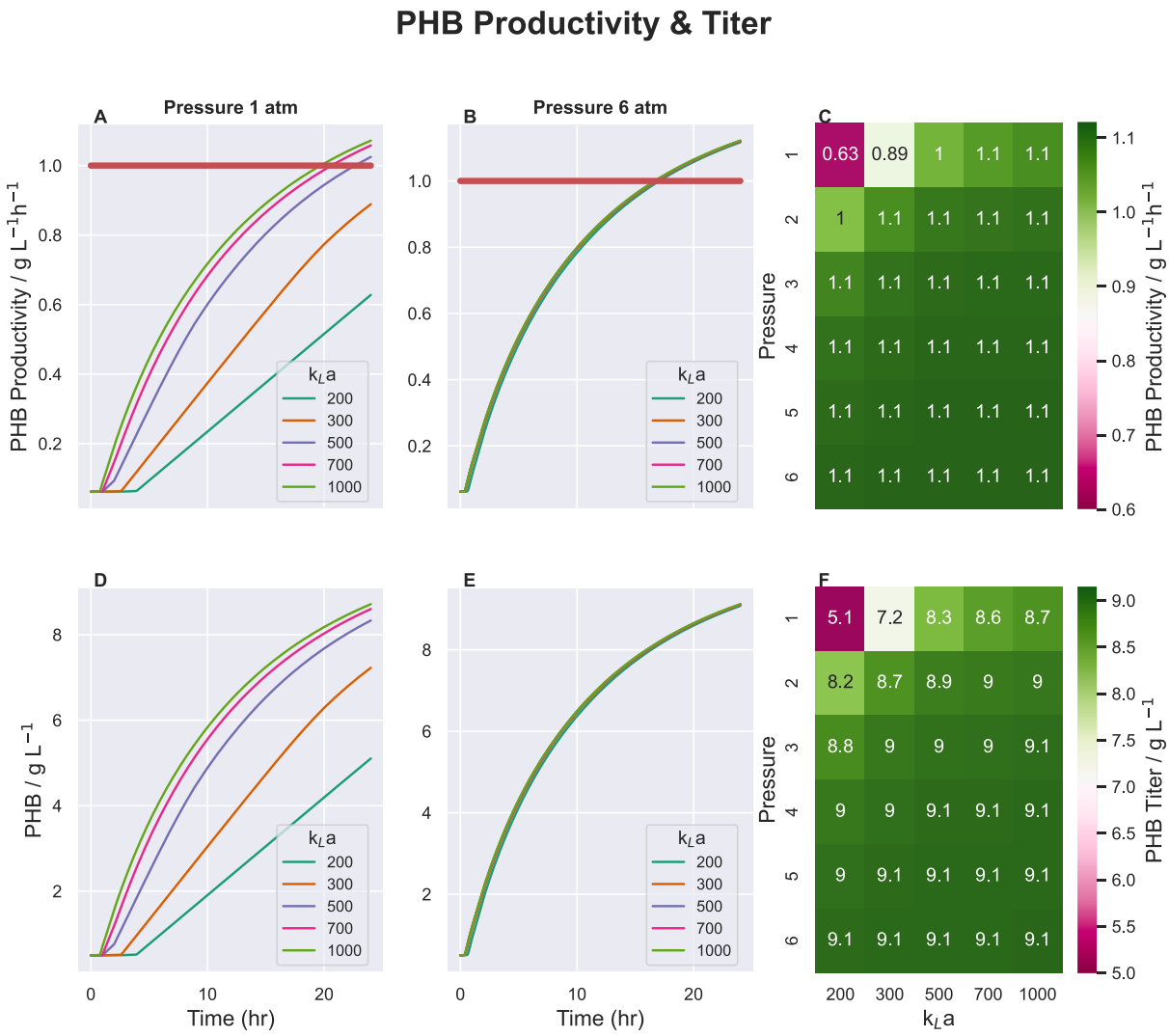

Fig. 3. Coupled effects of mass transfer rate (k_La) and pressure on PHB productivity (A–C) and titer (D–F). All *in-silico* experiments assume nitrogen limitation and an initial biomass concentration of 10 gL^{-1}.

of grams per liter hour for the biological conversion of methane to liquid fuels [40]. Typical bioreactor pressure values range from 1 to 6 atmospheres. From our simulations, we see that above 2 atmospheres there is not a significant increase in titer or productivity.

The only parameters that vary for this numerical study are k_La (e.g., 200–1000 [h^{-1}]) and total pressure (e.g., 1–6 [atm]), all other reactor conditions remain unchanged. Table 4 summarizes resulting Da numbers associated with parametric sweep pairs. Over the sweep range, reaction rates are high relative to mass transfer rates, indicating that factors that increase reaction rate (e.g., an increase in partial pressure of influent CH_4 or O_2, or an increase in trace copper for maximum methane monooxygenase activity) is expected to have a greater impact on PHB productivity.

Fig. 3 shows PHB productivity and accumulation, along with corresponding heatmaps from the parametric sweep. A pressure at the low and high ends of the simulations is shown for comparison, the data are then aggregated into a dataframe and a heatmap generated to show all parametric sweep pairs and their resulting values.

Each panel in the first two columns of Fig. 3 contain curves for each of the k_La values used for the parametric sweep. The first column, Fig. 3. (A,D) shows a numerical study for a pressure of 1 atmosphere, with varying k_La. The second column, Fig. 3(B and E) is the same numerical study, but at a pressure of 6 atmospheres. While increasing either of these parameters increases PHB titer and productivity metrics, operation at a pressure exceeding 1 atmosphere is not necessary to achieve a PHB productivity on the order of grams per liter per hour (red horizontal bar in Fig. 3 (A and B)). The numerical experiments shown in Fig. 3 (B and E) show that k_La curves overlap at a pressure of 6 [atm]. These simulations demonstrate that when operating at high pressures (e.g., 6 [atm]), PHB productivity and titer are not necessarily limited by CH_4 bioavailability. Instead, these in-silico experiments suggest that PHB productivity and titer are limited by available nitrogen in the growth medium. The numerical experiments shown in Fig. 3(A and B) suggest that a continuous system (i.e. a CSTR) operating at a sufficient residence time could achieve productivity rates on the order of ~ 1 [$gL^{-1}h^{-1}$] in different ways, say, for example by operating at k_La values of 300 to 1000 h^{-1} at a pressure of 1 [atm]. This is further illustrated in Fig. 3(C) where PHB productivity rates are computed for a broad range of combinations of k_La and pressure, showing that pressures of 2 atmospheres and above will slightly surpass productivity rates of 1 [$gPHBL^{-1}h^{-1}$]. However, a pressure of 1 atmosphere with a k_La of 300 [h^{-1}] or above enables productivities near or at the level of grams per liter per hour, while at the same time reaching titer values near those of higher-pressure systems. Higher pressures will yield higher titer and productivity due to increased bioavailability of gaseous substrates. While high pressure systems have been used in the past to increase PHB productivity [11], these systems present increased explosion risks and require sophisticated monitoring to keep those risks low.

Fig. 3(F) illustrates titer across the parametric sweep of k_La and pressure. There is not a significant increase of PHB titer when considering pressures of 2 atmospheres and above. At a pressure of 1 atmosphere, increasing k_La improves titer by ~ 70 %. At a k_La of 200 [h^{-1}], increasing from 1 [atm] to 2 [atm] improves titer by ~ 60 %. An increase in k_La or pressure has the added benefit of increasing the bioavailability of CH_4 – either by increasing saturation concentration or by delivering CH_4 at a higher rate than can be consumed. Considering our DamKöhler analysis, for a k_La of 200 [h^{-1}], we note that the system is not necessarily limited by cell metabolism, but by mass transfer (Da ≫ 1). Keeping all other variables constant, pressure increases the saturation concentration of CH_4, and thus brings Da closer to unity. The same is true of increasing k_La, where an increase in the mass transfer rate increases the bioavailable mass of CH_4. Increasing bioavailability of CH_4 then becomes a key metric for bioreactor design. In a previous study we noted that increasing bioavailability of CH_4 can be achieved using unconventional gas delivery methods, such as membrane contactors or oils [41]. Increasing CH_4 saturation has implications for bioreactor design and may allow for operation at lower mass transfer rates and pressures, increasing overall energy efficiency.

3.2. Impacts of aqueous CO_2 from microbial activity and gas delivery on PHB productivity

Aqueous carbon dioxide (CO_2) can inhibit methanotrophic growth, especially at elevated pressures [19]. Wendlandt et al. 1993 developed biokinetic models (incorporated in Equation 1) to assess the impacts of aqueous CO_2 concentration, noting that elevated concentration levels hinder optimal growth. Moreover, without pH control, increased aqueous CO_2 decreases system pH, hindering microbial growth. Of interest is how aqueous CO_2, introduced via microbial activity and as a gaseous input, can impact growth and product accumulation at elevated pressures. For this base case analysis, mineral media is assumed to be sufficiently buffered to allow for an initial, optimal pH of 5.7 at a pressure of 1 [atm], and with a CO_2 gas composition of 10 % (no additional sources of buffer are added to adjust pH throughout the analysis). Methanotrophic growth and PHB accumulation typically require the same or similar environmental conditions for optimal performance. Using this assumption, the impacts of aqueous CO_2 concentrations are evaluated using the kinetic CO_2 and pH models developed by Wendlandt et al. 1993 and Rosso et al. 1995 [19,25]. In the subsequent simulations, CO_2 gas composition is varied from volume fractions of 10–50 %, k_La was maintained at a moderate value of 300 [h^{-1}], and pressure was varied from 1 to 6 atmospheres. CO_2 gas composition was varied to investigate the impacts of using gaseous streams that may have

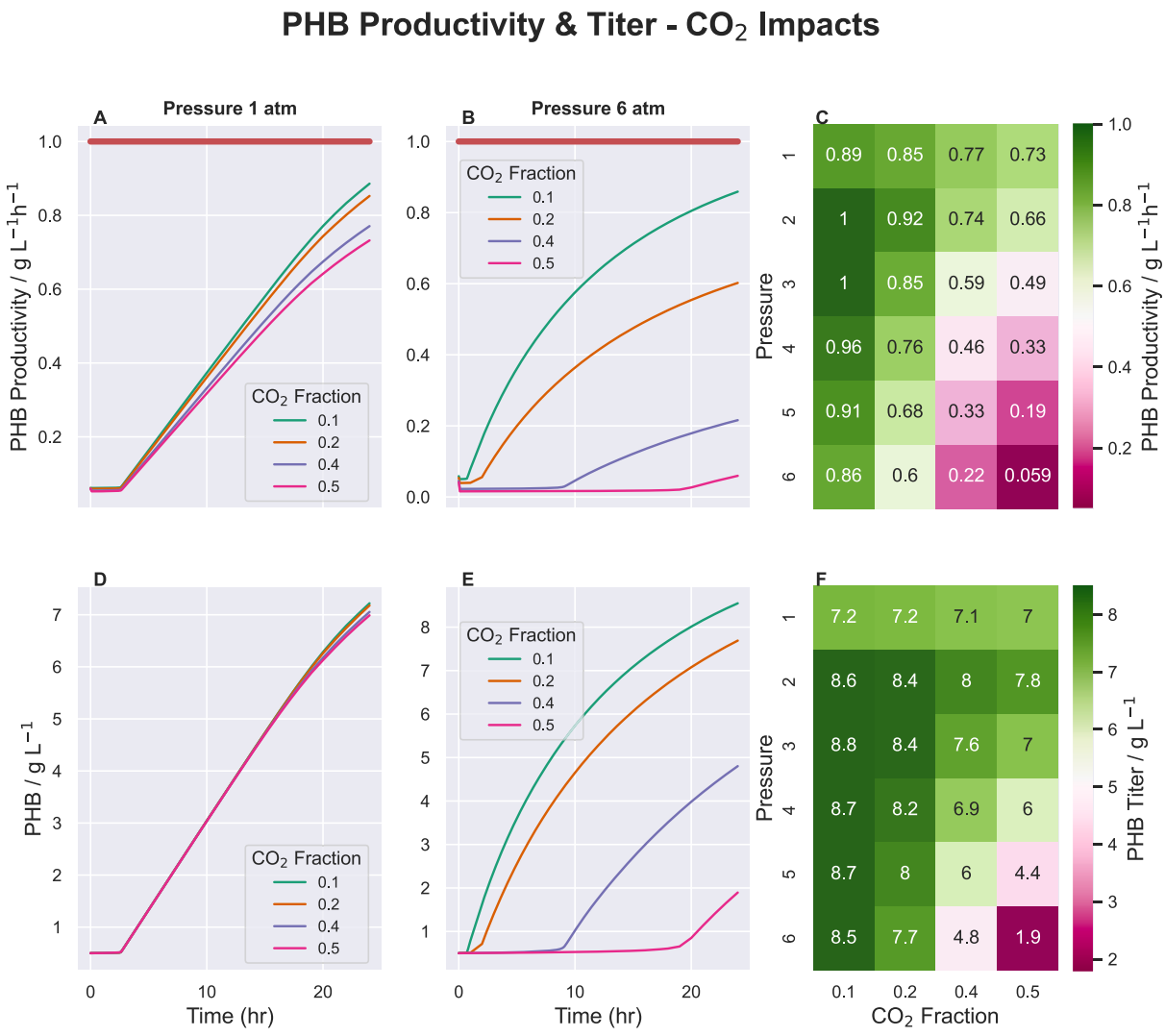

Fig. 4. Coupled effects of CO_2 and pressure on PHB productivity (A–C) and titer (D–F). All numerical experiments evaluated under a nitrogen limitation strategy and with a starting biomass concentration of 10 gL^{-1}.

up to 50 % CO_2, such as biogas from anaerobic digesters [42].

Fig. 4, similar to Fig. 3, shows PHB productivity and accumulation, evaluated at varying pressures, but this time considering aqueous CO_2 concentrations. Each panel of Fig. 4 shows the resulting PHB productivity (Fig. 4A–C) and titer (Fig. 4D–F) evaluated with CO_2 inhibition impacts. At elevated pressures, aqueous CO_2 concentrations begin to impact microbial performance. In this simulation the only parameters that vary are CO_2 volume fraction (%) and pressure, all other parameters are kept constant and are not impacted by other physics within the bioreactor.

Each panel in the first two columns of Fig. 4 contain curves for CO_2 fractions used in the parametric sweep. Similar to Fig. 3, we show numerical studies evaluated at pressures of 1 [atm] (Fig. 4(A and D)) and 6 [atm] (Fig. 4(B and E)) for comparison. While increasing pressure benefits productivity (Fig. 3), considering CO_2 concentrations at elevated pressures shows a decrease in achievable PHB productivity. This trend can be clearly seen in Fig. 4(C), where PHB productivity is computed for all parametric sweep pairs in this analysis. Operating at any pressure (in this analysis) and with a CO_2 gas fraction of 10 % shows that PHB productivity can reach a level of $\sim$ 1 [$gL^{-1}h^{-1}$], suggesting that CO_2 gaseous composition should be monitored to maintain this level of CO_2 in the gas phase. Inhibition due to pH and CO_2 are greater for systems operating at pressures of 3–6 [atm], and with CO_2 fractions $\geqslant$ 20 % where productivity decreases to a low of 0.06 [$gL^{-1}h^{-1}$]; at lower pressures $\leqslant$ 3 [atm] and with CO_2 fractions of 10 %, impacts are less pronounced, with productivity staying at or near the level of grams per liter per hour.

Combined effects of CO_2 and pH on PHB titer are summarized in Fig. 4(D–F). Again, CO_2 in the gas phase is varied from 10 to 50 %, CO_2 derived from microbial metabolism is considered, and pH is allowed to vary as a result of CO_2 gas–liquid mass transfer. As pressures increase in these systems, the saturation concentration of CO_2 increases, impacting pH and ultimately microbial performance. A similar, decreasing trend is seen in achievable PHB titer as pressure and CO_2 volume fraction increase. A system operating at a pressure of 6 [atm] and with a CO_2 volume fraction of 50 % shows a $\sim$ 4.5-fold decrease in PHB titer as compared to a similar system operating with a CO_2 volume fraction of 10 %. This analysis is significant in determining how best to operate a pressurized vessel using feed streams that potentially contain elevated levels of gaseous CO_2, such as biogas. Biogas is an attractive feedstock as it would be readily available at wastewater treatment plants fitted with anaerobic digesters or landfills, where the alternatives would be to flare excess CH_4 or use it as an energy source to power plant operations. Given an economically feasible way to control CO_2 composition, diverting biogas to a methanotrophic bioreactor for PHB production is an attractive alternative to generate a sustainable product while at the same time mitigating release of harmful greenhouse gases.

Ultimately, high productivity and titer are needed for cost effective scale-up. Operation at high pressures will require close monitoring of CO_2 and buffer for pH control. Low to moderate values for k_La, pressures of 2–3 [atm], and CO_2 volume fractions of 10–20 % could enable acceptable bioreactor performance.

3.3. Bioreactor heat transfer rate

Methanotrophic respiration is highly exothermic, releasing metabolic heat when cells are cultivated at high density, regardless of whether cells are replicating or accumulating PHB [22]. Maintenance of a productive and efficient process requires heat management. Typical bioreactor processes rely upon cooling jackets or baths that maintain desired temperatures. Such systems rely upon transfer of heat from growing cells to a coolant, typically water, which is circulated through a heat exchanger. In lab scale experiments, temperature in shake flasks and climate-controlled chambers is held constant, and at low biomass concentrations (<5 [$g_{vss}L^{-1}$]), cooling is not typically required. As active microbial biomass concentrations increase, however, cooling costs increase, and measures to control the release of metabolic heat are needed to maintain high levels of productivity and efficiency.

Fig. 5 illustrates the effects of heat transfer rates (i.e., cooling capability) on bioreactor performance for a pressure of 1 [atm], a k_La of 300 [h^{-1}], and an initial biomass concentration of 10 [gL^{-1}]. Typical forced convection processes function at overall heat transfer rates of $\sim$ 10–20,000 [$Wm^{-2}°C^{-1}$] using either cooling air or cooling water [43]. To determine an optimal range of heat transfer rates, the sole heat source is assumed to be microbial metabolic activity, and the reactor is assumed to be completely mixed, such that temperature is uniform throughout the reactor. In the following analysis low, moderate, and high heat transfer rates of 1, 10, and 100 [$Wm^{-2}°C^{-1}$] are considered.

As shown in Fig. 5. (A, B), low to moderate heat transfer rates do not allow for optimal ranges of productivity or titer. Low heat transfer rates result in low PHB titer, $\sim$3 [gL^{-1}], and essentially no productivity due to increases in system temperature, which lead to sub-optimal microbial performance. For a heat transfer rate on the order of 100 [$Wm^{-2}°C^{-1}$], productivity increases from $\sim$ 0.35 [$gL^{-1}h^{-1}$] to $\sim$ 0.9 [$gL^{-1}h^{-1}$]. This rate also has significant impacts on titer, where sufficient cooling suggests a $\sim$ 2.5-fold increase in achievable titer, Fig. 5. (B). As shown in Fig. 5. (A, C), a heat transfer rate of 100 [$Wm^{-2}°C^{-1}$] is sufficient for productive and efficient operation, with PHB productivity near the level of grams per liter per hour and with an energy efficiency in the range of 19–20 %. Higher energy efficiency is achievable due to increased levels of PHB production, which are a result of adequate bioreactor heat removal. Increasing k_La to a value of 400 [h^{-1}], with sufficient heat

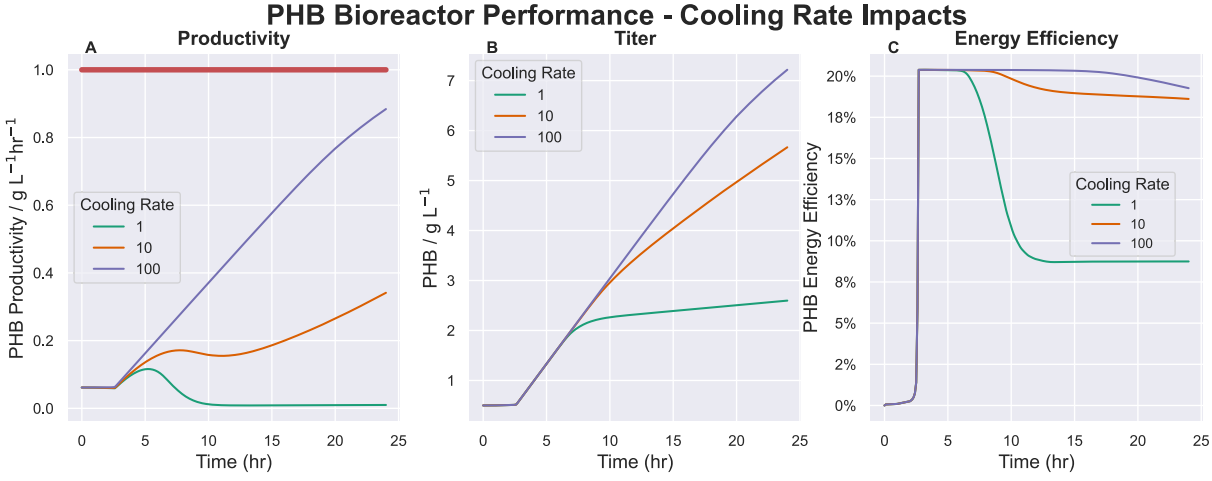

Fig. 5. Impacts of bioreactor heat transfer rate on PHB Productivity (A), Titer (B), & Energy Efficiency (C).

removal, increases productivity by ~ 10 % with a ~ 2 % decrease in overall energy efficiency. These increases in productivity and titer have implications for reactor design and overall process costs, specifically pertaining to bioreactor sizing, geometry, and mixing requirements.

Low productivity systems require larger bioreactors to achieve high final biomass [gL^{-1}] concentrations with high PHB content (P_{max}), comparable to high productivity systems. These bioreactors increase system costs, which increases the cost of the final product, in this case, PHB, making it challenging to compete economically with traditional petroleum-based plastics. Systems-level costs are best evaluated with a techno-economic analysis (TEA), where a sensitivity analysis would indicate which parameters impact cost most significantly. Systems-level process models can be used to determine optimal bioreactor operation strategies and minimum cooling rates while still maintaining efficient operation. While this analysis reveals that heat transfer rates on the order of 100 [$Wm^{-2}°C^{-1}$] would provide sufficient cooling for our specific system, future models should consider more elaborate reactor geometries, in addition to considering heat sources from mechanical processes such as mixing.

3.4. Impacts of mass transfer & microbial kinetic parameters on productivity and energy efficiency

Increasing the energy efficiency of PHB production is critical for scale-up and competition with traditional petroleum-based plastic manufacturing facilities. Considerable energy is required to increase mass transfer of hydrophobic gas substrates into aqueous media. Fig. 6 shows the energy efficiencies and productivities of PHB accumulation for mass transfer at moderate and high rates and key stoichiometric and kinetic parameters for PHB production, such as PHB yield, $Y_{p_{CH4}}$, and the PHB to active biomass ratio, P_{max}. Not considered is the energy required for cooling the system, in which case, η_{PHB} is taken as an upper bound. The following analysis highlights literature reported values of PHB yield and P_{max} for mixed methanotrophic consortiums, pure cultures, and a hypothetical case where a mixed consortium exhibits P_{max} values similar to pure cultures. The microbial parameters used in this analysis have been observed for pure ($Y_{p_{CH4}}$=0.52 [$gPHBgCH_4^{-1}$], P_{max} = 0.486 [−]) and mixed cultures ($Y_{p_{CH4}}$=0.8 [$gPHBgCH_4^{-1}$], P_{max} = 0.34 [−]) of methanotrophic organisms [11,44]. Ranges for yield (active biomass and PHB) and P_{max} can vary significantly, causing considerable variability in η_{PHB}.

In each panel of Fig. 6, solid lines are energy efficiency or productivity evaluated under conditions where $Y_{p_{CH4}}$ is either 0.8 [$gPHBgCH_4^{-1}$] (upper bound for mixed consortiums) or 0.52 [$gPHBgCH_4^{-1}$] (*Methylocystis* GB 25) with a P_{max} of 0.34 [−]. The dashed lines are energy efficiency and productivity evaluated under conditions where P_{max} changes to a value of 0.486 [−]. Fig. 6(A) illustrates PHB energy efficiency evaluated at a k_La of 300 [h^{-1}], showing a maximum energy efficiency close to 30 %, and tapering off to ~ 28 % when $Y_{p_{CH4}}$ = 0.8 [$gPHBgCH_4^{-1}$] and P_{max} = 0.486 [−]. In this scenario, an upper bound on energy efficiency is observed given that a methanotrophic organism exhibits PHB yield characteristics similar to a mixed culture and PHB accumulation similar to a pure culture. In the same panel we can see that a pure culture with a $Y_{p_{CH4}}$ = 0.52 [$gPHBgCH_4^{-1}$] and P_{max} = 0.486 [−] has an upper bound of energy efficiency close to 20 %, then tapering off to ~ 19 %. When evaluated with mixed culture characteristics, $Y_{p_{CH4}}$ = 0.8 [$gPHBgCH_4^{-1}$] and P_{max} = 0.34 [−], energy efficiency tapers off to ~ 16 %. A similar decreasing trend in energy efficiency (~13 %) can be seen if pure cultures are to exhibit lower PHB accumulation capabilities. Increasing yield on PHB alone has the potential to increase energy efficiency by up to 45 % – illustrating the importance of selecting

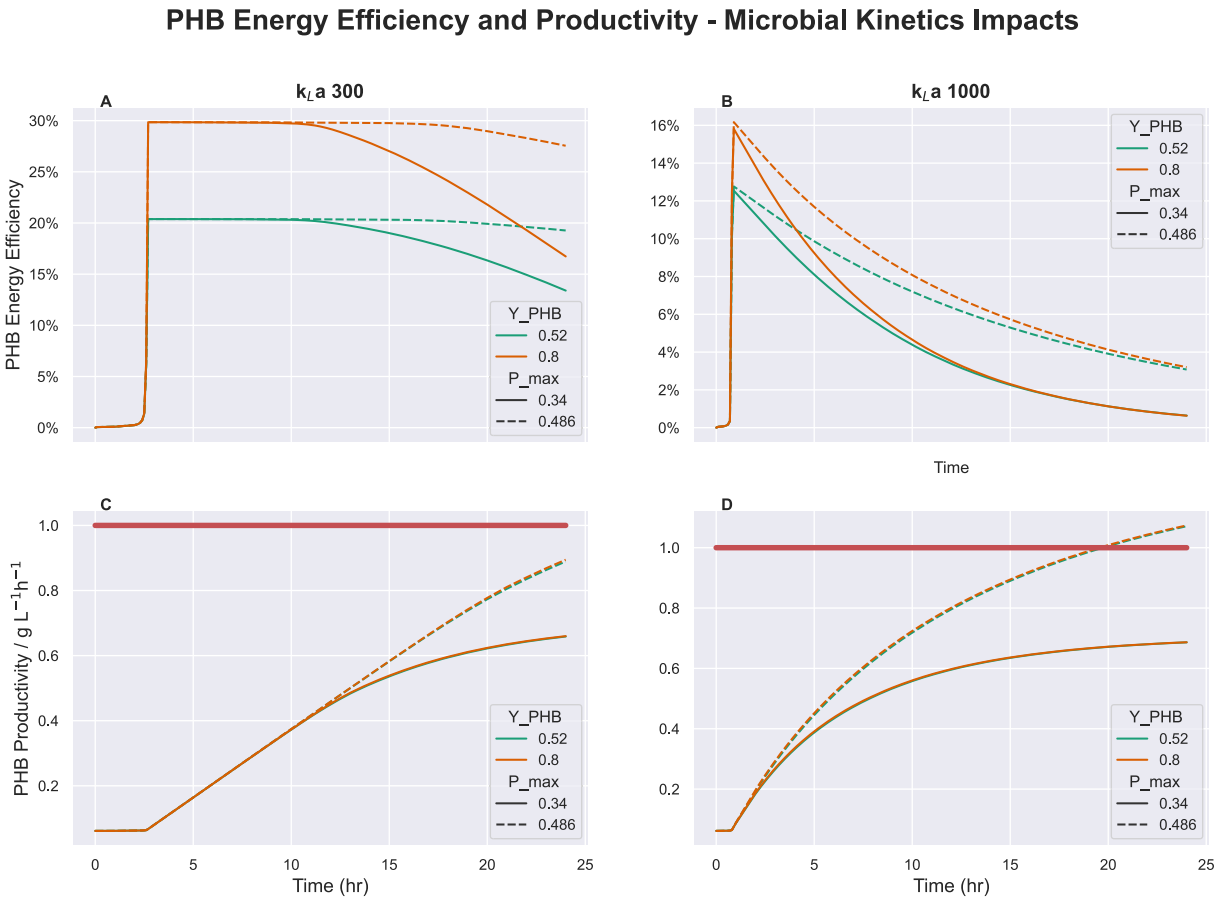

Fig. 6. Coupled effects of k_La and microbial kinetics of energy efficiency and productivity.

Table 5
Energy efficiency and productivity metrics.

k_La [h^{-1}]	Y_{PHB} [$gPHBgCH_4^{-1}$]	P_{max} [−]	Energy Efficiency Range [%]	Productivity [$gPHBL^{-1}h^{-1}$]
300	0.52	0.486	19–20	0.90
300	0.8	0.486	28–30	0.90
300	0.52	0.34	13–20	0.66
300	0.8	0.34	17–30	0.66
1000	0.52	0.486	3–13	1.07
1000	0.8	0.486	3–16	1.07
1000	0.52	0.34	<2–13	0.68
1000	0.8	0.34	<2–16	0.68

organisms that have a high PHB yield. While this has yet to be observed, an energy analysis can potentially guide experimental design when working with pure or mixed cultures. For example, given that mixed cultures show relatively high PHB yields, researchers may try to selectively grow these organisms to exhibit higher PHB content within the cells either by metabolic or genetic engineering or by inducing selective environmental stressors (e.g., heat shock, multiple nutrient deficiency, high ionic strength, etc.). Working with mixed microbial cultures has the added benefit of reducing or completely eliminating the need for PHB production in sterile, controlled environments; removing this requirement ultimately decreases overall process costs [45,46].

In Fig. 6(B) energy efficiency is evaluated in a similar fashion, with the exception of assuming that a bioreactor is operated at a high mass transfer rate of 1000 [h^{-1}]. Energy efficiency tapers off quickly from a high of ~ 16 % to a low value of ~ 3 %, considering PHB yield characteristics similar to a mixed culture with PHB accumulation similar to that of a pure culture. In the scenario where P_{max} is 0.486 [−], having high ($Y_{p_{CH4}}$=0.8 [$gPHBgCH_4^{-1}$]) or moderate ($Y_{p_{CH4}}$=0.52 [$gPHBgCH_4^{-1}$]) PHB yields give the same result of ~ 3 % energy efficiency. Considering P_{max} of 0.34 [−] yields energy efficiency results for both PHB yield cases below ~ 2 %. Because methanotrophs grow and accumulate PHB relatively quickly at high mass transfer rates, k_La dominates our continuous energy efficiency analysis. The tradeoff is that systems can be operated continuously in a highly productive manner (e.g., >1 [$gL^{-1}h^{-1}$]), see Fig. 6(D). To evaluate the impacts of doing so would require a life-cycle assessment (LCA) and techno-economic analysis (TEA). With these tools, bioplastics practitioners can further evaluate what energy efficiency means to them and their eventual partners or customers.

In Fig. 6(C and D) productivity is evaluated to illustrate the impact of microbial kinetic parameters on PHB productivity. In both panels (C,D) PHB content, P_{max}, plays a critical role in PHB productivity. At a k_La of 300 [h^{-1}], a high productivity on the order of grams per liter per hour, is close to achievable whether an organism exhibits high PHB yield ($Y_{p_{CH4}}$=0.8 [$gPHBgCH_4^{-1}$]) or a moderate PHB yield ($Y_{p_{CH4}}$=0.52 [$gPHBgCH_4^{-1}$]) when P_{max} is 0.486. Interestingly, a low P_{max} results in an upper bound of productivity rates of ~ 0.66 [$gPHBL^{-1}h^{-1}$]. A relatively high P_{max} of 0.486 [−] increases productivity to ~ 0.9 [$gPHBL^{-1}h^{-1}$], a productivity increase of ~ 36 %. A similar trend, with higher overall productivity rates is predicted at a k_La of 1000 [h^{-1}], where a low and high P_{max} result in productivities of ~ 0.68 [$gPHBL^{-1}h^{-1}$] and 1.07 [$gPHBL^{-1}h^{-1}$], respectively. The latter is a productivity increase of ~ 57 %. Pertinent metrics from this analysis are summarized in Table 5.

When coupled to the energy efficiency analysis, decisions can be made regarding continuous operation and PHB production. At high productivities, systems can be operated at moderate mass transfer rates and within a range of energy efficiencies (13–30 %), depending on microbial kinetic characteristics. The difference in productivity (relative to a mass transfer rate of 1000 [h^{-1}]), ~19 %, is significant and should be considered in tandem with achievable energy efficiency as these technologies scale. Assuming that all bioavailable CH_4 is consumed, Fig. 6 illustrates that increasing energy efficiency of PHB production with methanotrophs can be accomplished by 1) decreasing overall mass transfer rate, 2) increasing PHB yield on CH_4 or 3) increasing the PHB content within methanotrophic biomass. A tradeoff associated with increasing energy efficiency comes in the form of a decrease in the overall mass transfer rate, which slightly decreases PHB productivity but may be more economically competitive.

4. Conclusions and future work

The metrics in Figs. 3–6 highlight the importance and value of systems level modeling for the design and operation of bioreactors for PHB production. These types of numerical experiments are helpful in determining optimal design criteria for bioreactor systems, and capture complex interactions among physicochemical processes and thermodynamic constraints that are not readily apparent. While many experimental studies focus on design of high pressure and high mass transfer systems, we show here that these operating characteristics are not always required, and can in fact hinder process efficiency. Avoiding high pressure reactor systems reduces risks associated with highly compressed, explosive gaseous mixtures. At the same time, operating these systems at low to moderate mass transfer rates decreases energy costs, while increasing the energy efficiency of converting CH_4 to the target product, PHB, further decreasing overall process costs. The ability to operate these systems efficiently has implications for scaling of this technology as an effective CH_4 sink. Process optimization and efficiency for biological conversion of CH_4 into useful bioproducts is critical for the development of systems that can compete with conventional fossil carbon-based polymer manufacturing, while at the same time mitigating continued and excessive release of potent greenhouse gases. Subsequent modeling should consider how designs can be optimized for efficiency and costs, while minimizing negative climate change effects.

Declaration of Competing Interest

The authors declare that they have no known competing financial interests or personal relationships that could have appeared to influence the work reported in this paper.

Data availability

Data will be made available on request.

Acknowledgements

This work was supported by the Center for the Utilization of Biological Engineering in Space (CUBES) through NASA Award No. 1208377-1-RFATP. J. L. Meraz was supported by the Stanford Bio-X Bowes Graduate Student Fellowship and the Graduate Scholar in Residence Fellowship provided by Stanford's El Centro Chicano y Latino. A. J. Abel was supported by an NSF Graduate Research Fellowship under grant number DGE 1752814. We thank Dr. Hector Lopez-Hernandez for their mentorship, guidance, and helpful discussions regarding model development. The authors acknowledge this research was performed on the ancestral land of the Muwekma Ohlone Tribe. This land was and continues to be of great importance to the Ohlone people. Consistent with our values of community and inclusion, we have a responsibility to acknowledge, honor, and make visible the University's relationship to Native peoples.

Appendix A. Supplementary data

Supplementary data to this article can be found online at https://doi.org/10.1016/j.cej.2022.140166.

References

[1] D.T.N. Nguyen, O.K. Lee, T.T. Nguyen, E.Y. Lee, Type II methanotrophs: A promising microbial cell-factory platform for bioconversion of methane to chemicals, Biotechnol. Adv. 47 (2021), 107700.

[2] R.J. Conrado, R. Gonzalez, Chemistry envisioning the bioconversion of methane to liquid fuels, Science 343 (6171) (2014) 621–623.

[3] Q. Fei, M.T. Guarnieri, L. Tao, L.M.L. Laurens, N. Dowe, P.T. Pienkos, Bioconversion of natural gas to liquid fuel: opportunities and challenges, Biotechnol. Adv. 32 (3) (2014) 596–614.

[4] P.J. Strong, S. Xie, W.P. Clarke, Methane as a resource: can the methanotrophs add value? Environ. Sci. Technol. 49 (7) (2015) 4001–4018.

[5] M. Michalak, A.A. Marek, J. Zawadiak, M. Kawalec, P. Kurcok, Synthesis of PHB-based carrier for drug delivery systems with pH-controlled release, Eur. Polym. J. 49 (12) (2013) 4149–4156.

[6] H.-F. Listewnik, K.-D. Wendlandt, M. Jechorek, G. Mirschel, Process design for the microbial synthesis of poly-β-hydroxybutyrate (PHB) from natural gas, Eng. Life Sci. 7 (3) (2007) 278–282.

[7] J. Myung, M. Kim, M. Pan, C.S. Criddle, S.K.Y. Tang, Low energy emulsion-based fermentation enabling accelerated methane mass transfer and growth of poly(3-hydroxybutyrate)-accumulating methanotrophs, Bioresour. Technol. 207 (2016) 302–307.

[8] E.R. Sundstrom, C.S. Criddle, M.A. Elliot, Optimization of methanotrophic growth and production of poly(3-hydroxybutyrate) in a high-throughput microbioreactor system, Appl. Environ. Microbiol. 81 (14) (2015) 4767–4773.

[9] K.A. Stone, M.V. Hilliard, Q.P. He, J. Wang, A mini review on bioreactor configurations and gas transfer enhancements for biochemical methane conversion, Biochem. Eng. J. 128 (2017) 83–92.

[10] J. Myung, W.M. Galega, J.D. Van Nostrand, T. Yuan, J. Zhou, C.S. Criddle, Long-term cultivation of a stable Methylocystis-dominated methanotrophic enrichment enabling tailored production of poly(3-hydroxybutyrate-co-3-hydroxyvalerate), Bioresour. Technol. 198 (2015) 811–818.

[11] K.-D. Wendlandt, M. Jechorek, J. Helm, U. Stottmeister, Producing poly-3-hydroxybutyrate with a high molecular mass from methane, J. Biotechnol. 86 (2) (2001) 127–133.

[12] K.-D. Wendlandt, M. Jechorek, J. Helm, U. Stottmeister, Production of PHB with a high molecular mass from methane, Polym. Degrad. Stab. 59 (1-3) (1998) 191–194.

[13] M.S.I. Mozumder, L. Garcia-Gonzalez, H. De Wever, E.I.P. Volcke, Poly (3-hydroxybutyrate)(PHB) production from CO2: model development and process optimization, Biochem. Eng. J. 98 (2015) 107–116.

[14] M.S.I. Mozumder, L. Goormachtigh, L. Garcia-Gonzalez, H. De Wever, E.I. P. Volcke, Modeling pure culture heterotrophic production of polyhydroxybutyrate (PHB), Bioresour. Technol. 155 (2014) 272–280.

[15] D.E.G. Trigueros, C.L. Hinterholz, M.L. Fiorese, G.M.F. Aragão, W. Schmidell, M.A. M. Reis, A.D. Kroumov, Statistical evaluation and discrimination of competing kinetic models and hypothesis for the mathematical description of poly-3 (hydroxybutyrate) synthesis by Cupriavidus necator DSM 545, Chem. Eng. Sci. 160 (2017) 20–33.

[16] M. Moradi, H. Rashedi, S.R. Mofradnia, K. Khosravi-Darani, R. Ashouri, F. Yazdian, Polyhydroxybutyrate production from natural gas in a bubble column bioreactor: simulation using COMSOL, Bioengineering (Basel). 6 (2019), https://doi.org/10.3390/bioengineering6030084.

[17] X. Chen, Y. Rodríguez, J.C. López, R. Muñoz, B.-J. Ni, G. Sin, Modeling of Polyhydroxyalkanoate Synthesis from Biogas by Methylocystis hirsuta, ACS Sustainable Chem. Eng. 8 (9) (2020) 3906–3912.

[18] J. Helm, K.-D. Wendlandt, G. Rogge, U. Kappelmeyer, Characterizing a stable methane-utilizing mixed culture used in the synthesis of a high-quality biopolymer in an open system, J. Appl. Microbiol. 101 (2) (2006) 387–395.

[19] K.-D. Wendlandt, M. Jechorek, E. Brühl, The influence of pressure on the growth of methanotrophic bacteria, Acta Biotechnol. 13 (2) (1993) 111–115.

[20] J.A. Asenjo, J.S. Suk, Microbial Conversion of Methane into poly-β-hydroxybutyrate (PHB): Growth and intracellular product accumulation in a type II methanotroph, J. Ferment. Technol. 64 (1986) 271–278.

[21] J.A. Asenjo, J.S. Suk, Kinetics and models for the bioconversion of methane into an intracellular polymer, poly-β-hydroxybutyrate (PHB), Biotechnol. Bioeng. Sympos. (1986) 225–234.

[22] S.H. El Abbadi, C.S. Criddle, Engineering the dark food chain, Environ. Sci. Technol. 53 (5) (2019) 2273–2287.

[23] K.H. Rostkowski, A.R. Pfluger, C.S. Criddle, Stoichiometry and kinetics of the PHB-producing Type II methanotrophs Methylosinus trichosporium OB3b and Methylocystis parvus OBBP, Bioresour. Technol. 132 (2013) 71–77.

[24] S. Park, L. Hanna, R.T. Taylor, M.W. Droege, Batch cultivation of Methylosinus trichosporium OB3b. I: Production of soluble methane monooxygenase, Biotechnol. Bioeng. 38 (1991) 423–433.

[25] L. Rosso, J.R. Lobry, S. Bajard, J.P. Flandrois, Description of the combined effect of temperature and pH on the microbial growth by a convenient model, Appl. Environ. Microbiol. 61 (1995) 610–616.

[26] J. Helm, Methanotrophic bacteria as producers of poly (beta-hydroxybutyric acid) (PHB)-characterization of the process, the polymer and the stable mixed culture, Tech. Univ. Desden, Faculty of Mechanical Engineering, doctoral thesis, 2002.

[27] J.A. Asenjo, Bioreactor System Design, 1st ed., CRC Press, 1994.

[28] S.H. El Abbadi, E.D. Sherwin, A.R. Brandt, S.P. Luby, C.S. Criddle, Displacing fishmeal with protein derived from stranded methane, Nat. Sustain. 5 (1) (2022) 47–56.

[29] A.J. Abel, D.S. Clark, A comprehensive modeling analysis of formate-mediated microbial electrosynthesis, ChemSusChem 14 (1) (2021) 344–355.

[30] J.A. Amaral, T. Ren, R. Knowles, Atmospheric methane consumption by forest soils and extracted bacteria at different pH values, Appl. Environ. Microbiol. 64 (7) (1998) 2397–2402.

[31] R.E. Treybal, Mass transfer operations, Third Edition, McGraw-Hill, 1981.

[32] B. De heyder, P. Vanrolleghem, H. Van Langenhove, W. Verstraete, Kinetic characterization of mass transfer limited biodegradation of a low water soluble gas in batch experiments–necessity for multiresponse fitting, Biotechnol. Bioeng. 55 (3) (1997) 511–519.

[33] E.L. Cussler, Diffusion: Mass Transfer in Fluid Systems, Cambridge University Press, 2009.

[34] K. Van't Riet, Review of measuring methods and results in nonviscous gas-liquid mass transfer in stirred vessels, Ind. Eng. Chem. Proc. Des. Dev. 18 (1979) 357–364.

[35] A. Rohatgi, WebPlotDigitizer - Extract data from plots, images, and maps, (n.d.). https://automeris.io/WebPlotDigitizer (accessed July 21, 2022).

[36] D.N. Moriasi, J.G. Arnold, M.W. Van Liew, R.L. Binger, R.D. Harmel, T.L. Veith, Model Evaluation Guidelines for Systematic Quantification of Accuracy in Watershed Simulations, American Society of Agricultural and Biological Engineers, 2007.

[37] C. Tays, M.T. Guarnieri, D. Sauvageau, L.Y. Stein, Combined effects of carbon and nitrogen source to optimize growth of proteobacterial methanotrophs, Front. Microbiol. 9 (2018) 2239.

[38] B. Dam, S. Dam, Y. Kim, W. Liesack, Ammonium induces differential expression of methane and nitrogen metabolism-related genes in Methylocystis sp. strain SC2, Environ. Microbiol. 16 (10) (2014) 3115–3127.

[39] W. Van Hecke, R. Bockrath, H. De Wever, Effects of moderately elevated pressure on gas fermentation processes, Bioresour. Technol. 293 (2019), 122129.

[40] C.A. Haynes, R. Gonzalez, Rethinking biological activation of methane and conversion to liquid fuels, Nat. Chem. Biol. 10 (5) (2014) 331–339.

[41] J.L. Meraz, K.L. Dubrawski, S.H. El Abbadi, K.-H. Choo, C.S. Criddle, Membrane and fluid contactors for safe and efficient methane delivery in methanotrophic bioreactors, J. Environ. Eng. 146 (2020) 03120006.

[42] Y. Li, C.P. Alaimo, M. Kim, N.Y. Kado, J. Peppers, J. Xue, C. Wan, P.G. Green, R. Zhang, B.M. Jenkins, C.F.A. Vogel, S. Wuertz, T.M. Young, M.J. Kleeman, Composition and toxicity of biogas produced from different feedstocks in California, Environ. Sci. Technol. 53 (19) (2019) 11569–11579.

[43] P.M. Doran, Bioprocess Engineering Principles, Academic Press, 2013.

[44] P. Strong, B. Laycock, S. Mahamud, P. Jensen, P. Lant, G. Tyson, S. Pratt, The Opportunity for high-performance biomaterials from methane, Microorganisms 4 (1) (2016) 11.

[45] N. Gurieff, P. Lant, Comparative life cycle assessment and financial analysis of mixed culture polyhydroxyalkanoate production, Bioresour. Technol. 98 (17) (2007) 3393–3403.

[46] K.-D. Wendlandt, U. Stottmeister, J. Helm, B. Soltmann, M. Jechorek, M. Beck, The potential of methane-oxidizing bacteria for applications in environmental biotechnology, Eng. Life Sci. (2010).